Food Hydrocolloids 23 (2009) 1895–1902

Contents lists available at ScienceDirect

Food Hydrocolloids

journal homepage: www.elsevier.com/locate/foodhyd

Chitosan/clay films' properties as affected by biopolymer and clay micro/nanoparticles' concentrations

A. Casariego [a,b], B.W.S. Souza [a], M.A. Cerqueira [a], J.A. Teixeira [a], L. Cruz [c], R. Díaz [b], A.A. Vicente [a,*]

[a] IBB – Institute for Biotechnology and Bioengineering, Center of Biological Engineering, Universidade do Minho, Campus de Gualtar, 4710-057 Braga, Portugal
[b] Instituto de Farmacia y Alimentos, Universidad de la Habana, Ave. 23, No. 21425, entre 214 y 222, La Lisa CP 13600, Ciudad de La Habana, Cuba
[c] Facultad de Ingeniería Química, Instituto Superior Politécnico "José Antonio Echeverría", Ave. 114, Nº 11901, entre 119 y 127, Marianao CP 19390, Ciudad de La Habana, Cuba

ARTICLE INFO

Article history:
Received 31 July 2008
Accepted 3 February 2009

Keywords:
Chitosan
Clay
Micro/nanocomposite
Gas permeability
Mechanical properties
Thermal properties

ABSTRACT

Blends of chitosan (from Cuban lobster) and clay micro/nanoparticles were prepared by dispersion of the clay particles in the film matrix and the films obtained were characterized in terms of water solubility, water vapor, oxygen and carbon dioxide permeability, optical, mechanical and thermal properties using an Instron universal testing machine, differential scanning calorimetry, thermogravimetric analyses and scanning electron microscopy (*SEM*). The water vapor barrier properties of the films were significantly improved by incorporation of clay in their composition, while the water solubility decreased as the clay concentration increased (for a constant chitosan concentration). The tensile strength of chitosan/clay films increased significantly with increasing chitosan and clay concentrations, while the values of elongation decreased slightly for high values of chitosan concentration. T_m increased with the increase of chitosan concentration, but the changes in T_m with the addition of clay were not significant.
Polynomial models were fitted to the experimental data in order to facilitate future design of chitosan/clay film systems.

1. Introduction

The interest in the study of biopolymer films has witnessed a steady increase because they are environmentally friendly alternatives to synthetic, non-biodegradable films. They can retard moisture migration and the loss of volatile compounds, reduce the respiration rate, and delay changes in textural properties. Such films have been used to coat different products such as mandarin, cherry and strawberries (Fornes, Almela, Abad, & Manuel Agustí, 2005; Martínez-Romero et al., 2006; Ribeiro, Vicente, Teixeira, & Miranda, 2007).

They are also excellent barriers to fats and oils, and have a high selective gas permeability ratio CO_2/O_2 as compared to conventional synthetic films (Gontard, Thibault, Cuq, & Guilbert, 1996). However, their water vapor barrier properties are, in general, poor.

In the last years polymer/clay composites have received much attention, because of their extraordinary possibility to improve the barrier properties of thin films. These composites are a class of hybrid materials composed of organic polymer matrices and micro/nanoscale organophilic clay fillers (Kim, Lee, Oh, & Lee, 2003) and due to their high aspect ratios and high surface area, if clay particles are properly dispersed in the polymer matrix at a loading level of 1–5% (w/w) unique combinations of physical and chemical properties will be obtained, that turn these composites attractive for making films and coatings for a variety of industrial applications (Rhim, Hong, Park, & Perry, 2006).

Chitosan is the N-deacetylated form of chitin although this N-deacetylation is almost never complete. Most of the naturally occurring polysaccharides, e.g. cellulose, dextran, pectin, alginic acid, agar, agarose and carrageenans, are neutral or acidic in nature, whereas chitin and chitosan are examples of highly basic polysaccharides. Due to this unique property many potential products using chitosan have been developed, including flocculating agents for water and waste water treatment, chelating agents for removal of traces of heavy metals from aqueous solutions, coatings to improve dyeing characteristics of glass fibers, wet strength additives for paper, adhesives, photographic and printing applications, thickeners, and fibers and films (Hench, 1998).

Cuban coasts are very rich in lobsters, and therefore the fishing industry is a very important sector of activity. Furthermore, most of the lobster is locally processed and exported, being their carapaces a left over which can be used to obtain chitosan with different degrees of deacetylation. Chitosan films obtained with chitosan derived from crab and shrimp have been extensively studied (Alvarado et al., 2007; Butler, Vergano, Testin, Bunn, & Wiles, 1996;

* Corresponding author. Tel.: +351 253 604419; fax: +351 253 678986.
E-mail address: avicente@deb.uminho.pt (A.A. Vicente).

0268-005X/$ – see front matter © 2009 Elsevier Ltd. All rights reserved.
doi:10.1016/j.foodhyd.2009.02.007

Caner, Vergano, & Wiles, 1998; Hirano, 1989; Kittur, Haris, Udaya, & Tharanathan, 2002; Miranda, Garnica, Lara, & Cárdenas, 2004; Park, Marsh, & Rhim, 2002; Rhim et al., 2006; Xu, Ren, & Milford, 2006); given its economical relevance to the country, the characterization of lobster chitosan is needed, once it has been used successfully in the medical industry as well as for some applications in the food industry (Casariego et al., 2008; Cervera, Heinämäki, Krogars, et al., 2004; Cervera et al., 2005). The objective of this work is therefore to determine the effects of chitosan and clay concentrations on the barrier, mechanical, optical and thermal properties of chitosan films containing clay micro/nanoparticles in view of their possible use in the food and medical industries. This kind of applications will increase the added value of the products.

2. Materials and methods

The materials used to prepare the chitosan/clay films were: chitosan (obtained in the Pharmaceutical Laboratories Mario Muñoz, Cuba) with a degree of deacetylation of 90% approximately, lactic acid (Merck, Germany), micro/nanoclay particles (courtesy of Instituto Politécnico de Viana do Castelo, Portugal) with a mean particle size distribution of 2 μm (and ca. 20% of the particles <100 nm) and distilled water.

2.1. Micro/nanocomposite film preparation

The chitosan solutions were prepared dissolving the chitosan (1.0, 1.5 or 2.0% w/v) in a 1% (v/v) lactic acid solution using a magnetic stirrer during 2 h at room temperature (20 °C).

Micro/nanoclay (MNC) particles' suspensions (in 1 and 3% w/w chitosan) were prepared according with the methods reported by Xu et al. (2006) by dispersing appropriate amounts of MNC into 5 mL of 1% lactic acid solution and vigorously stirring for 24 h. Afterwards, 100 mL of the appropriate chitosan solution were added slowly into the pretreated MNC suspensions. The mixtures were stirred continuously for 4 h and then 28 mL were cast onto glass Petri dishes. The films were dried in an oven at 35 °C during 8 h. Dried films were peeled from the plate and cut in circles with approximately 80 mm diameter for further testing.

2.2. Characterization of chitosan/clay films

2.2.1. Water solubility

The film solubility in water was determined according to the method reported by Cuq, Gontard, Cuq, and Guilber (1996). It was defined by the content of dry matter solubilized after 24 h immersion in water. The initial dry matter content of each film was determined by drying to constant weight in an oven at 105 °C. Two disks of film (2 cm diameter) were cut, weighed, and immersed in 50 mL of water. After 24 h of immersion at 20 °C with occasional agitation, the pieces of film were taken out and dried to constant weight in an oven at 105 °C, to determine the weight of dry matter which was not solubilized in water. The measurement of solubility of the films was determined as follows:

$$SOL = \left(M_i - M_f\right)/M_i \times 100 \quad (1)$$

where SOL is the percentage of soluble material, M_i is the initial mass and M_f is the final mass of the sample.

2.2.2. Permeability to gases

The water vapor permeability (WVP) of the films was determined gravimetrically based on ASTM E96-92 method (Guillard, Broyart, Bonazzi, Guilbert, & Gontard, 2003; McHugh, Avena-Bustillos, & Krochta, 1993). The test film was sealed on the top of a permeation cell containing distilled water (100% RH; 2.337×10^3 Pa vapor pressure at 20 °C), placed in a desiccator which was maintained at 20 °C and 0% RH (0 Pa water vapor pressure) with silica gel. The water transferred through the film and adsorbed by the desiccant was determined from weight loss of the permeation cell. The cups were weighed at intervals of 2 h during 10 h. Steady-state and uniform water pressure conditions were assumed by keeping the air circulation constant outside the test cup by using a fan inside the desiccator (McHugh et al., 1993). The slope of weight loss versus time was obtained by linear regression. The measurement (WVP) of the films was determined as follows:

$$WVP = (WVTR \cdot L)/\Delta P \quad (2)$$

where $WVTR$ is the measured water vapor transmission rate (g/$m^{-2}\,s^{-1}$) through the film, L is the mean film thickness (m), and ΔP is the partial water vapor pressure difference (Pa) across the two sides of the film. For each type of film, WVP measurements were replicated three times.

Oxygen permeability (O_2P) and carbon dioxide permeability (CO_2P) were determined based on the ASTM (2002) method. A chitosan film was sealed between two chambers, having each one two channels (one for gas inlet and one for gas outlet). In the lower chamber O_2 or CO_2 was supplied at a controlled flow rate to keep the pressure constant in that compartment. The other chamber was purged by a stream of nitrogen, also at a controlled flow rate. This nitrogen acted as a carrier for the O_2 or CO_2 and the flow leaving this chamber was connected to an O_2 sensor. The flows of the two chambers were connected to a manometer to ensure the equality of pressures between both compartments (1 atm in each). As the O_2 or CO_2 crossing the film was carried continuously by the nitrogen flow, it was considered that O_2 or CO_2 partial pressure in the upper compartments was null, therefore ΔP was at all times equal to 1 atm. Oxygen permeability (O_2P) was determined based on the measurement of O_2 concentration by the O_2 sensor, while carbon dioxide permeability (CO_2P) was determined measuring CO_2 concentration at the outlet of the upper compartment with a gas chromatograph (Chrompack 9001, Middelburg, Netherlands) where a column Porapak Q 80/100 mesh 2 m × 1/8″ × 2 mm SS was installed; the oven temperature was 35 °C, and the detector and injector temperature were both at 110 °C. The flow rate of the carrier gas was 23 mL/min.

All chitosan films used for permeability determinations were previously conditioned in desiccators at 20 °C and 25% RH.

2.2.3. Optical properties

The color of chitosan films was determined with a Minolta colorimeter (CR 300; Minolta, Japan). A white standard color plate ($Y = 93.5$, $x = 0.3114$, $y = 0.3190$) for the instruments' calibration was used as a background for color measurements of the coated films, and the CIE $L^*a^*b^*$ values of each film were evaluated by reflectance measurement (García, Pinotti, Martino, & Zaritzky, 2004). The opacity of a material is an indication of how much light passes through it. The higher the opacity, the lower the amount of light that can pass through the material. Generally, opacity is calculated from reflectance measurements. The opacity of the samples was determined according to the Hunter lab method, as the relationship between the opacity of each sample on a black standard (Y_b) and the opacity of each sample on a white standard (Y_w) (García & Sobral, 2005).

2.2.4. Mechanical properties: tensile strength (TS) and elongation-at-break (E)

TS and E were measured with an Instron Universal Testing Machine (Model 4500, Instron Corporation) following the guidelines of ASTM Standard Method D 882-91. The initial grip separation

was set at 30 mm and the crosshead speed was set at 5 mm/min. *TS* was expressed in MPa and calculated by dividing the maximum load (N) by the initial cross-sectional area (m^2) of the specimen. *E* was calculated as the ratio of the increased length to the initial length of a specimen (30 mm) and expressed as a percentage. *TS* and *E* tests were replicated five times for each type of film.

*2.2.5. Differential scanning calorimetry (*DSC*)*

Differential scanning calorimetry (*DSC*) measurements were performed with a Shimadzu DSC-50 (Shimadzu Corporation, Kyoto, Japan) calibrated with Indium as standard. Ca. 10 mg of the samples were placed in aluminium DSC pans (Al crimp Pan C.201-52943). The samples were heated from 25 to 350 °C at a heating rate of 10 °C/min under helium atmosphere (Cervera, Heinämäki, Krogars, et al., 2004; Cervera, Heinämäki, Räsänen, et al., 2004; Nunthanid, Puttipipatkhachorn, Yamamoto, & Peck, 2001).

2.2.6. Thermal stability analysis

Thermogravimetric analyses (*TGA*) were completed with a Shimadzu TGA-50 (Shimadzu Corporation, Kyoto, Japan). Samples were placed in the balance system and heated from 25 °C to 600 °C at a heating rate of 10 °C/min under a helium atmosphere.

*2.2.7. Scanning electron microscopy (*SEM*)*

Scanning electron microscopy (*SEM*) was used to examine the surface of chitosan films. Pieces were cut from films and were mounted directly on stubs, freeze dried and coated with gold. Samples were examined and photographed under a scanning electron microscope (LEICA S 360) with the build films Image Analyzing System, for an accelerating voltage of 15 kV.

2.2.8. Film thickness

Film thickness was measured with a hand-held digital micrometer (Mitutoyo, Japan) having a sensitivity of 0.001 mm. This measurement was carried out at the end of the permeability test to avoid the effect of mechanical damage that could be caused on the film during the thickness measurement. Ten thickness measurements were taken on each testing sample in different points and the mean values were used in permeability calculations.

2.2.9. Statistical analyses

All data were analyzed and compared by using ANOVA and Duncan Multiples Range test ($\alpha = 0.05$) to determine the significance of differences, on Statgraphics Plus version 5.1 software (Statistical Graphics Corp, 2000, USA).

The data related to the influence of MNC and chitosan concentration on the water solubility, water vapor, oxygen and carbon dioxide permeability and mechanical properties of MNC/chitosan films were adjusted with polynomial models (Eq. (3)) and independent variables were codified according to a multifactor design

$$Y = b_0 + b_1 q + b_2 c + b_3 q^2 + b_4 c^2 + b_5 (q \cdot c) \quad (3)$$

where *Y* is the dependent variable (*WS*, *MC*, *WVP*, *OP*, CO_2P, *TS* or *E*), *q* is chitosan concentration (1.0, 1.5 and 2.0% w/v) and *c* is MNC concentration (1.0 and 3.0% w/w chitosan). The values of b_0–b_5 are model coefficients.

Table 1
Effect of chitosan and clay concentrations on the moisture content and water solubility of chitosan/MNC particles' films (mean values (standard deviation); $\alpha = 0.05$).

Factors		Moisture content (%)	Water solubility (%)
Chitosan concentration (% w/v)	MNC particles' concentration (% w/w chitosan)		
1.0	0	26.54 ± 0.06^{e}	46.50 ± 1.86^{b}
1.0	1	25.18 ± 0.12^{de}	42.59 ± 5.89^{a}
1.0	3	27.15 ± 2.21^{e}	38.11 ± 1.33^{a}
1.5	0	23.13 ± 0.34^{d}	52.31 ± 1.11^{b}
1.5	1	19.25 ± 0.43^{c}	41.49 ± 6.29^{a}
1.5	3	18.97 ± 2.22^{c}	37.60 ± 1.80^{a}
2.0	0	14.84 ± 0.19^{b}	93.88 ± 5.23^{e}
2.0	1	13.32 ± 0.59^{ab}	74.44 ± 3.13^{c}
2.0	3	11.33 ± 0.71^{a}	86.08 ± 2.87^{d}

Different letters in the same column correspond to statistically different samples for a 95% confidence level.

3. Results and discussion

3.1. Water solubility and moisture content

Water solubility is a measure of the resistance of a film sample to water. The results obtained (Table 1) showed that the water

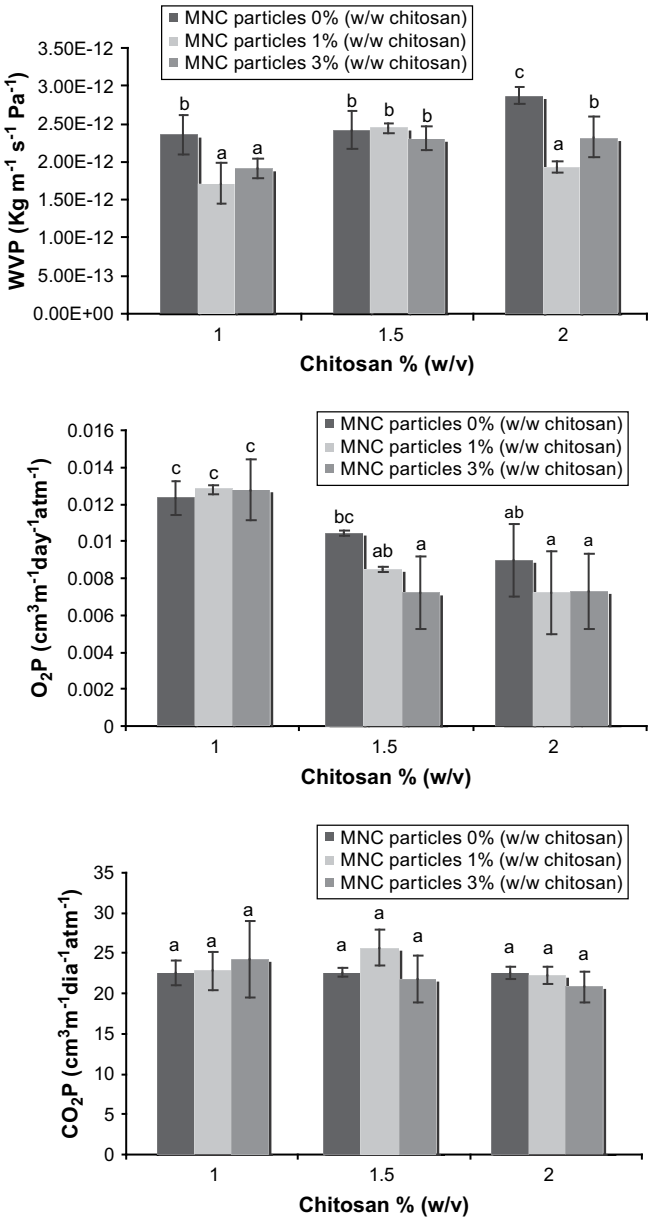

Fig. 1. Barrier properties (*WVP*, O_2P and CO_2P) as a function of chitosan and MNC particles' concentration on chitosan/MNC particles' films produced with 1.0% (v/v) lactic acid (average ± confidence interval, $\alpha = 0.05$).

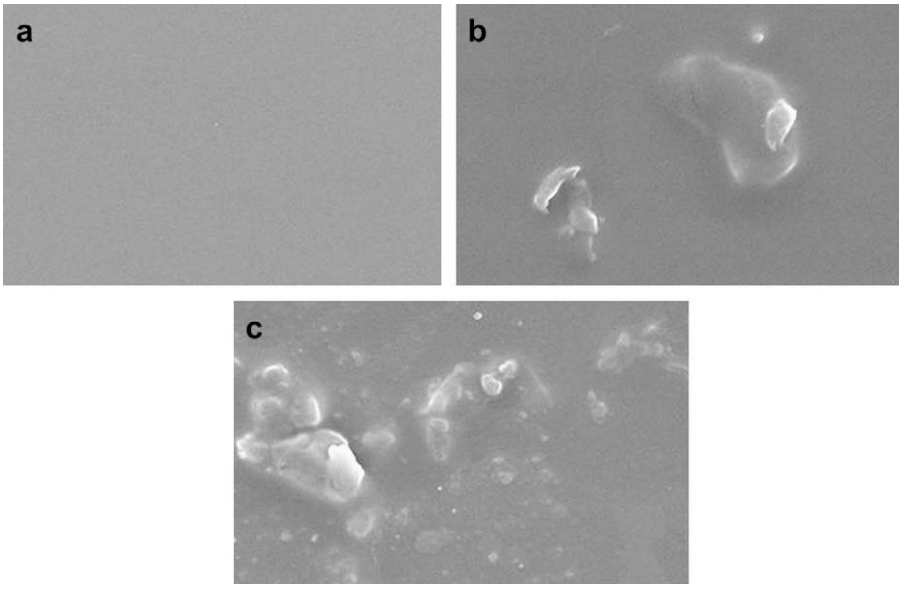

Fig. 2. SEM photographs of the surface of chitosan/MNC particles' films (magnification = 3600×): (A) films with 2% (w/v) chitosan; (B) films with 2% chitosan (w/v) and 1% MNC particles (w/w chitosan); (C) films with 2% (w/v) chitosan and 3% MNC particles (w/w chitosan).

solubility decreased as the clay concentration increased keeping chitosan concentration constant ($p \leq 0.05$); such decrease is very substantial for films containing 2% (w/v) chitosan, which is a clear indication that the chitosan concentration is the variable which most influences water solubility. This is confirmed by the following polynomial model (Eq. (4)), to which the data were fitted following the procedure described in Materials and methods. The model also shows that there is some moderate interaction among clay particles and chitosan, which could explain the chitosan molecules in the films are some irregularities in the general behaviors, such as the one observed between the case of 2% (w/v) chitosan and 1% MNC and that of 1.5% (w/v) chitosan and 1% MNC.

$$WS = 39.551 + 19.820q + 20.891q^2 + 3.894q{\cdot}c \quad (p \leq 0.05); \quad R^2 = 0.982 \tag{4}$$

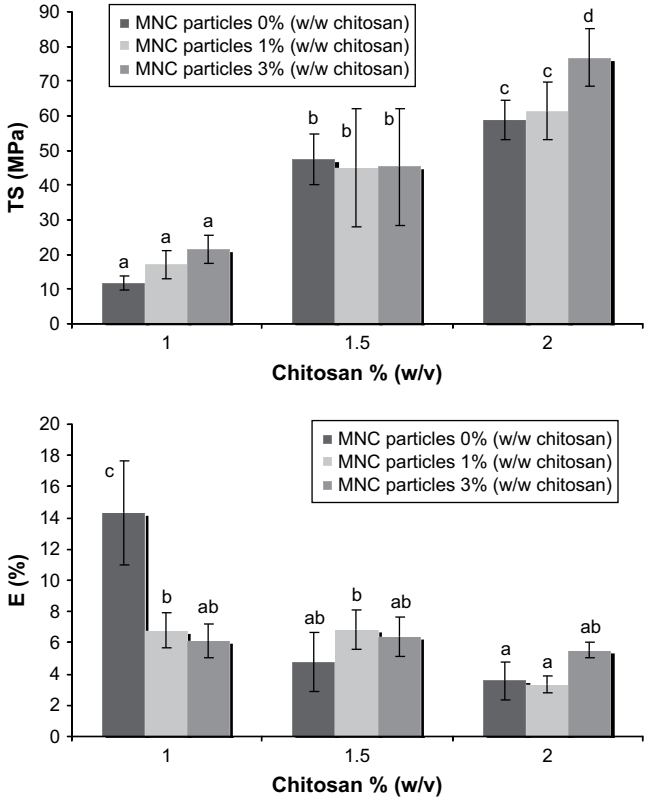

Fig. 3. Mechanical properties of chitosan/MNC particles' films.

Chitosan films have a higher affinity for water compared with the powder, probably because protonated, rendering the films more hydrophilic than the powder itself (Cervera, Heinämäki, Krogars, et al., 2004; Lim & Wan, 1995). This may justify in part the increase of water solubility for increasing chitosan concentrations in the films. In fact, this is patent from the model (Equation (4)), where clearly chitosan concentration is the most important factor influencing *WS*. Also, as can be seen from the results in Table 1, there is a decrease in the moisture content of chitosan films prepared from the 2% chitosan FFS with the increase of clay particles' concentration, presumably due to the presence of clay in the films. This influence of the clay in the films will be even higher after drying the FFS, once the mass of chitosan in each film keeps being the same and the mass of water is reduced.

The moisture content decreased with an increase of clay and chitosan concentrations ($p \leq 0.05$); which is represented by:

$$MC = 19.096 - 6.924q - 0.985q{\cdot}c \quad (p \leq 0.05); \quad R^2 = 0.962 \tag{5}$$

3.2. Water vapor permeability

The *WVP* values of the chitosan and chitosan-based composite films containing MNC particles are shown in Fig. 1. The water vapor barrier property of the films was significantly improved by incorporation of MNC in the film matrix ($p \leq 0.05$). The greatest values of *WVP* were obtained for those films with the lowest concentration of chitosan and a significant influence of both chitosan and clay concentrations ($p \leq 0.05$) on *WVP* was found. The *WVP* values of the chitosan films (1.0–2.0% w/v) ranged between 1.75×10^{-12} kg m $(m^2\ s\ Pa)^{-1}$ and 2.94×10^{-12} kg m $(m^2\ s\ Pa)^{-1}$; the values are higher

Table 2
Color parameters of chitosan/clay films (mean values (standard deviation); $\alpha = 0.05$).

Factors		L^*	a^*	b^*	ΔE^*
MNC particles (% w/w chitosan)	Chitosan concentration (% w/v)				
0	1	94.24 (0.64)^{f}	3.42 (0.20)^{ab}	12.25 (1.09)^{b}	11.65 (1.25)^{a}
0	1.5	92.70 (0.39)^{bc}	3,65 (0.20)^{b}	12.76 (1.82)^{b}	15.71 (0.64)^{b}
0	2	91.02 (0.99)^{a}	4,07 (0.70)^{c}	17.76 (0.62)^{c}	21.65 (2.37)^{c}
1	1	93.67 (0.16)^{de}	4.19 (0.26)^{c}	9.66 (1.08)^{a}	13.53 (1.04)^{a}
1	1.5	92.52 (0.62)^{bc}	3.68 (0.26)^{b}	11.67 (1.96)^{b}	15.82 (2.05)^{b}
1	2	93.07 (0.40)^{cd}	3.17 (0.16)^{a}	12.76 (1.66)^{b}	16.76 (1.69)^{b}
3	1	94.08 (0.38)^{ef}	4.11 (0.35)^{c}	7.91 (0.66)^{a}	11.75 (0.64)^{a}
3	1.5	92.30 (0.52)^{b}	3.63 (0.21)^{b}	12.67 (1.26)^{b}	16.84 (1.37)^{b}
3	2	92.87 (0.42)^{bc}	3.22 (0.17)^{a}	13.18 (1.53)^{b}	17.20 (1.58)^{b}

Different letters in the same column correspond to statistically different samples for a 95% confidence level.

than those reported by Rhim et al. (2006), for chitosan films at 2% (w/v) in a solution of acetic acid 1% (w/v) (1.31×10^{-12} kg m (m^2 s Pa)$^{-1}$). This difference could be due either to the acid used to dissolve the chitosan or because we used chitosan obtained from lobster instead of chitosan from another source. The *WVP* of the composite films decreased significantly ($p \leq 0.05$) by 9–32% depending on the chitosan and clay concentrations. Rhim et al. (2006) reported that the *WVP* of composite films decreased significantly ($p < 0.05$) by 25–30% depending on the nanoparticles used; these values compare well with the values obtained in the present work.

Although the *WVP* values of chitosan film decreased upon compositing with nanoparticles, they are still not comparable to those of widely used plastic films.

The decrease in *WVP* of nanocomposite films is believed to be due to the presence of ordered dispersed nanoparticle layers with large aspect ratios in the polymer matrix (Cussler, Highes, Ward, & Aris, 1998; Yano, Usuki, & Okad, 1997). This forces water vapor traveling through the film to follow a tortuous path through the polymer matrix surrounding the particles, thereby increasing the effective path length for diffusion (Rhim et al., 2006).

The influence of clay concentration on *WVP* depends on the type of composites formed (tactoids, intercalation and exfoliation). Intercalation and exfoliation are two ideal nanoscale composites, the formation of which depends on the types and amounts of nanoclay used (Xu et al., 2006). In the present work it is possible that clay particles were exfoliated, as Fig. 2 seems to indicate, that is, the MNC particles were dispersed throughout the chitosan matrix, and these results are similar to those reported by Rhim et al. (2006). Nevertheless it is necessary to continue working in this aspect, by means of the employment of other techniques such as AFM, which allow the definition of the degree of interaction between the particles of clay and chitosan.

Data in Fig. 1 were fitted to a polynomial model (Eq. (6)) the fitting coefficients suggesting that chitosan concentration is the variable of higher influence.

$$WVP = 2.43 \times 10^{-12} + 1.8 \times 10^{-13} q - 4 \times 10^{-13} q^2 + 2.3 \times 10^{-13} q^2 \cdot c \quad (p \leq 0.05); \quad R^2 = 0.80 \tag{6}$$

3.3. Oxygen (O_2P) and carbon dioxide (CO_2P) permeability

Many previous studies of chitosan films with acetic acid reported their lower O_2P (Butler et al., 1996; Muzzarelli, Isolati, & Ferrero, 1974). The values of O_2P for chitosan films are comparable with those of existing commercial synthetic films such as those of polyvinylidene chloride (PVDC) or ethylene vinyl alcohol copolymer films (Butler et al., 1996). However, chitosan films with lactic acid have equal or lower values of O_2P.

In the present work, the values of O_2P oscillated in the range 7.4–13.1×10^{-3} $cm^3\, O_2\, m^{-1}\, day^{-1}\, atm^{-1}$ (Fig. 3); these values are similar to those reported by Caner et al. (1998), who obtained O_2P values of 4.42 and 0.19×10^{-3} $cm^3\, O_2\, m^{-1}\, day^{-1}\, atm^{-1}$ for 3% (w/w) chitosan films with 1% and 7.5% lactic acid, respectively. These authors evaluated the effect of type and concentration of acid on the O_2P and found that lactic acid containing films were those having the lowest values, followed by acetic, propionic, and formic acid.

The results obtained (Fig. 1) showed that the O_2P decreased as the increased chitosan concentration ($p \leq 0.05$) and the chitosan concentration showed a significant effect ($p \leq 0.05$). This is clear from the model equation obtained for O_2P data (Eq. (7)).

$$O_2P = 0.0081 - 0.0028q + 0.0221q^2 \quad (p \leq 0.05); \quad R^2 = 0.954 \tag{7}$$

Chitosan and MNC particles' concentration does not seem to influence significantly CO_2P ($p \leq 0.05$) (Fig. 1).

However, it is certain that the use of the clay did not allow improving this property, neither affected its CO_2 barrier properties.

3.4. Optical properties

The results of the measurements of color are shown in Table 2. All of the films were transparent, with a slight yellowish tint. With respect to the lightness (L^*) of the chitosan films, it is possible to observe that these values are relatively high in comparison with those of chitosan-based nanocomposites obtained by Rhim et al. (2006), for which the values range between 66.8 and 85.8, probably because they incorporated four types of nanoparticles in

Table 3
Opacity of chitosan/MNC particles' films (mean values (standard deviation), $\alpha = 0.05$).

Factors		Opacity (%)
Chitosan concentration (% w/v)	MNC particles' concentration (% w/w chitosan)	
1.0	0	8.23 ± 1.09^{a}
1.0	1	11.28 ± 0.55^{a}
1.0	3	11.07 ± 0.73^{a}
1.5	0	8.20 ± 1.46^{a}
1.5	1	9.95 ± 0.65^{a}
1.5	3	9.71 ± 0.66^{a}
2.0	0	10.79 ± 0.72^{a}
2.0	1	9.89 ± 0.66^{a}
2.0	3	10.08 ± 0.66^{a}

Different letters in the same column correspond to statistically different samples for a 95% confidence level.

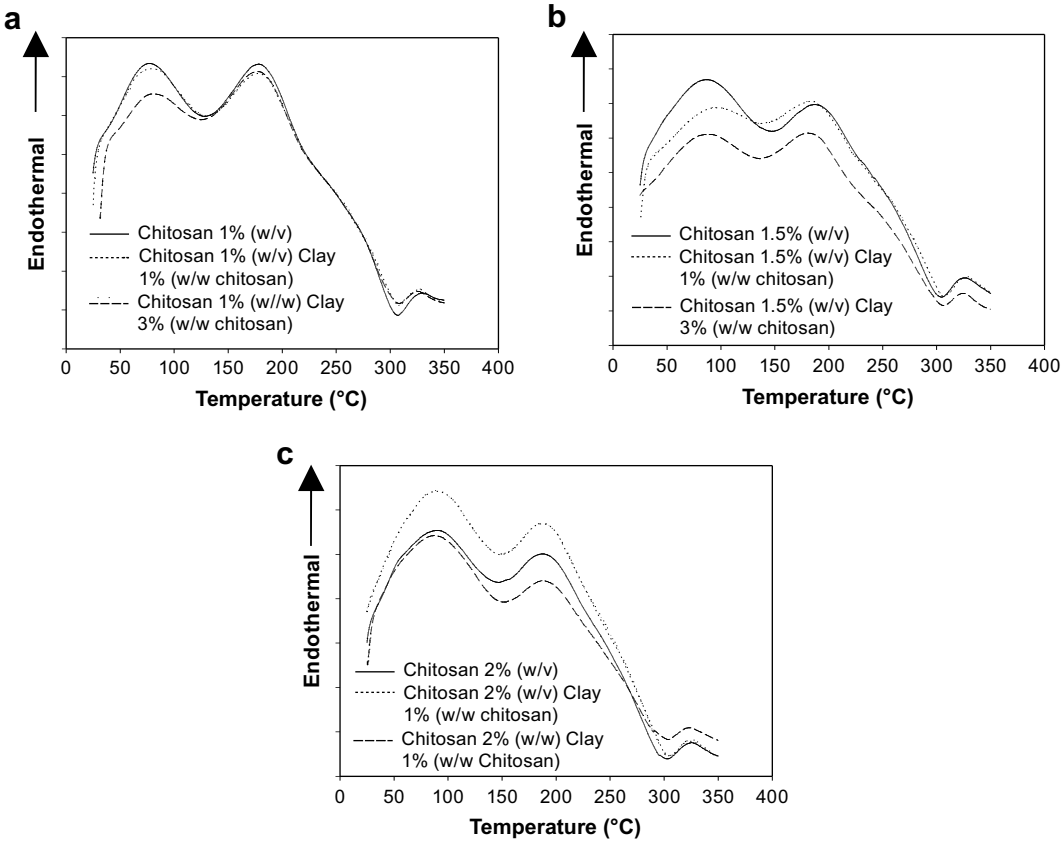

Fig. 4. DSC thermographs of chitosan/MNC particles' films, for different chitosan concentrations: a) 1.0% (w/v); b) 1.5% (w/v); c) 2.0% (w/v).

concentrations of 5% (w/w, relative to chitosan on a dry basis). Such films were reported to be transparent. Similar results were obtained with respect to the component b^{+*}, that is, our films were yellower than those reported by Rhim et al. (2006), probably because we use chitosan from a different source and obtained by a different procedure.

The results indicate that an increase in the concentration of the chitosan while keeping MNC particles' concentration constant tends to decrease the values of L^* and a^* and to increase the values of b^* ($p < 0.05$).

The b^* value is the parameter describing the color of chitosan-based films due to the natural yellowish color of chitosan, and it is the chromatic coordinate influencing the total color difference.

Park et al. (2002) reported values of 15.43 ± 2.32 and 16.65 ± 2.33 for b^* and ΔE^*, respectively, for chitosan films at 2% (w/v) in a solution of lactic acid 1%.

The transparency of a film is a desirable property once the consumer wishes to see clearly the aspect of the product which the film will cover. The opacity is an established measurement of the transparency of a film. A greater value of opacity means a smaller transparency (Cuq et al., 1996). The results presented in Table 3 clearly show that the presence of MNC particles does not affect the opacity of chitosan films, similar results to those of Rhim et al. (2006).

3.5. Mechanical properties

As can be observed in Fig. 3, the *TS* of chitosan/MNC particles' films increased significantly ($p < 0.05$) with increasing chitosan concentration; while the values of *E* (Fig. 3) decreased for high values of chitosan concentration. These results are in good agreement with previously reported values for chitosan films (Butler et al., 1996; Rhim et al., 2006).

Previous works have reported that *TS* values of chitosan/clay films increased significantly with increasing clay concentration due to a possible strain-induced alignment of the clay particle layers in the polymer matrix (Giannelis, 1996) and the strong interaction between the polymer matrix and silicate layers via the formation of hydrogen bonds (Sinha & Okamoto, 2003). However, in this work there was no significant influence of the clay concentration on the mechanical properties of the chitosan/MNC films. This behavior may be due to the lower values of clay concentration used, when compared to those of Giannelis (1996).

The values of *TS* and *E* of the films can be described by the following polynomial equations, respectively:

$$TS = 45.091 + 24.836q \quad (p \leq 0.05); \quad R^2 = 0.914 \tag{8}$$

$$E = 6.640 - 1.1017q - 1.186q^2 + 0.716q \cdot c \quad (p \leq 0.05); \quad R^2 = 0.758 \tag{9}$$

3.6. Differential scanning calorimetry and thermal stability

DSC plots of chitosan films are presented in Fig. 4. Two endothermic peaks were detected for all films. The first endothermic peak that occurs over the temperature range of 78–94 °C was attributed to solvent evaporation (Cervera, Heinämäki, Krogars, et al., 2004; Cervera, Heinämäki, Räsänen, et al., 2004; Lim & Wan, 1995; Xu et al., 2006), while the peaks in the range of 179–190 °C showed that crystallization of the chitosan was not inhibited by the

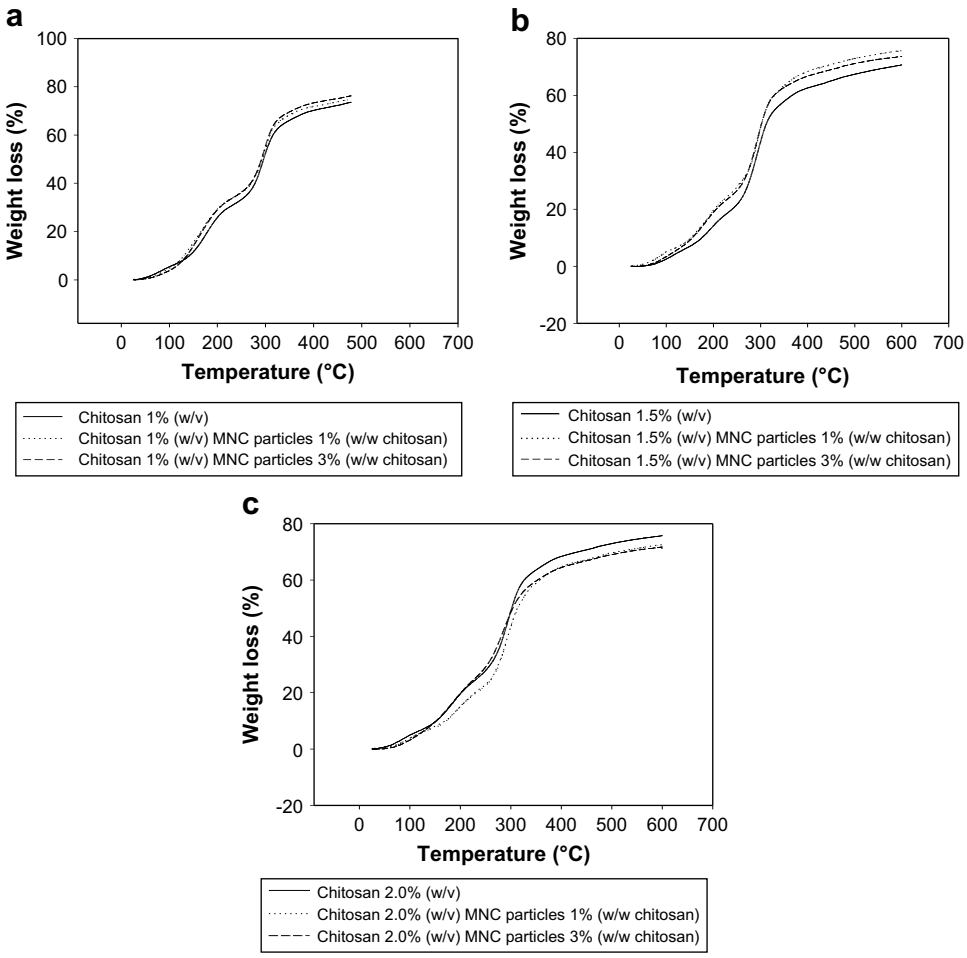

Fig. 5. TGA curves of chitosan/MNC particles' films, for different chitosan concentrations: a) 1.0% (w/v); b) 1.5% (w/v); c) 2.0% (w/v).

MNC particles, once there is no shift of this peak for increasing MNC particles' concentration.

T_m increased with the increase of chitosan concentration; also the changes in T_m, with addition of MNC particles, were not significant for the films considered, indicating that the crystal forms and structure of chitosan were not changed. Similar results were reported by Xu et al. (2006) with addition of *MMT*-Na^+ to chitosan films.

Changes in the thermal stability of chitosan/MNC particles' films were examined by *TGA*. The weight-loss curves of the films, as a function of temperature, are shown in Fig. 5. The onset temperatures of thermal degradation did not show significant variations among the chitosan films without and with MNC particles in their composition. All chitosan films were degraded at 286–297 °C, which agrees well with the results reported by Cervera, Heinämäki, Räsänen, et al. (2004) and Xu et al. (2006).

4. Conclusions

MNC particles were dispersed into a chitosan film matrix. The *WVP* of the films was reduced ($p < 0.05$) by incorporation of such particles, while the water solubility decreased as the clay concentration increased (for a constant chitosan concentration). The values of *TS* strength of chitosan/nanoclay films increased significantly ($p < 0.05$) with increasing chitosan concentration, while the values of *E* decreased for high values of chitosan concentration. The presence of clay does not seem to influence the values of those two properties. The values of T_m increased with the increase of chitosan concentration, but no significant changes in T_m were detected with the addition of clay. Mathematical model equations were developed in order to allow evaluating the behavior of the obtained chitosan/clay films.

Acknowledgements

The author A. Casariego is the recipient of a fellowship from the αLFA VALNATURA Project of Europe Aid Cooperation Office and the author B.W.S. Souza is the recipient of a fellowship from the Coordenação de Aperfeiçoamento de Pessoal de Nível Superior (CAPES, Brazil) and M.A. Cerqueira is recipient of fellowships from the Fundação para a Ciência e Tecnologia (FCT, Portugal) (SFRH/BD/23897/2005); both fellowships are gratefully acknowledged. We also wish to gratefully acknowledge Prof. António Labrincha from the Instituto Superior Politécnico de Viana do Castelo for the supply and characterization of the clay samples.

References

Alvarado, J. D., Almeida, A., Arancibia, M., Carvalho, R. A., Sobral, P. J. A., Habitante, A. M. Q. B., et al. (2007). Método directo para la obtención de quitosano de desperdicios de camarón para la elaboración de películas biodegradables. *Afinidad: Revista de Química Teórica y Aplicada, 64*(531), 605–611.

ASTM D 3985-02. (2002). Standard test method for oxygen gas transmission rate through plastic film and sheeting using a coulometric sensor. In *ASTM book of standards 15.09*.

Butler, B. L., Vergano, P. J., Testin, R. F., Bunn, J. M., & Wiles, J. L. (1996). Mechanical and barrier properties of edible chitosan film as affected by composition and storage. *Journal of Food Science, 61*(5), 953–961.

Caner, C., Vergano, P. J., & Wiles, J. L. (1998). Chitosan film mechanical and permeation properties as affected by acid, plasticizer and storage. *Journal of Food Science, 63*(6), 1049–1053.
Casariego, A., Souza, B. W. S., Vicente, A. A., Teixeira, J. A., Cruz, L., & Díaz, R. (2008). Chitosan coating surface properties as affected by plasticizer, surfactant and polymer concentrations in relation to the surface properties of tomato and carrot. *Food Hydrocolloids, 22*, 1452–1459.
Cuq, B., Gontard, N., Cuq, J. L., & Guilber, S. (1996). Functional properties of myofibrillar protein based biopackaging as affected by film thickness. *Journal of Food Science, 61*(3), 580–584.
Cussler, E. L., Highes, S. E., Ward, W. J., & Aris, R. (1998). Barrier membranes. *Journal of Membrane Science, 38*, 161–174.
Cervera, M. F., Heinämäki, J., Krogars, K., Jörgensen, A. M., Iraizoz, A., & Yliruusi, J. (2004). Solid-state and mechanical properties of aqueous chitosan–amylose starch films plasticized with polyols. *AAPS Pharmaceutical Science Technology, 5*(1) : article 15, 1–6.
Cervera, M. F., Heinämäki, J., Räsänen, M., Antikainen, O., Nieto, O. M., Iraizoz, A., et al. (2004). Determination of tackiness of chitosan film-coated pellets exploiting minimum fluidization velocity. *International Journal of Pharmaceutics, 281*, 119–127.
Cervera, M. F., Heinämäki, J., Salgado-Rodriguez, E., Antikainen, O., Iraizoz, A., & Yliruusi, J. (2005). Effective optimization of enteric film coating of pellets with a miniaturized top-spray coater. *Pharmazeutische Industrie, 67*(2), 231–236.
Fornes, F., Almela, V., Abad, M., & Manuel Agustí, M. (2005). Low concentrations of chitosan coating reduce water spot incidence and delay peel pigmentation of Clementine mandarin fruit. *Journal of the Science of Food and Agriculture, 85*, 1105–1112.
García, F. T., & Sobral, P. J. A. (2005). Effect of the thermal treatment of the filmogenic solution on the mechanical properties, color and opacity of films based on muscle proteins of two varieties of Tilapia. *LWT - Food Science and Technology, 38*, 289–296.
García, M., Pinotti, A., Martino, M. N., & Zaritzky, N. E. (2004). Characterization of composite hydrocolloid films. *Carbohydrate Polymers, 56*, 339–345.
Giannelis, E. P. (1996). Polymer layered silicate nanocomposites. *Advanced Materials, 8*, 29–35.
Gontard, N., Thibault, R., Cuq, B., & Guilbert, S. (1996). Influence of relative humidity and film composition on oxygen and carbon dioxide permeabilities of edible films. *Journal of Agricultural and Food Chemistry, 44*(4), 1064–1069.
Guillard, V., Broyart, B., Bonazzi, C., Guilbert, S., & Gontard, N. (2003). Preventing moisture transfer in a composite food using edible films: experimental and mathematical study. *Journal of Food Science, 68*(7), 2267–2277.
Hench, L. L. (1998). Biomaterials: a forecast for the future. *Biomaterials, 19*, 1419–1423.
Hirano, S. (1989). Production and application of chitin and chitosan in Japan. In A. Skjak-Braek, & Sanford. (Eds.), *Chitin and chitosan* (pp. 37–43). London: Elsevier Science Publishing Co.
Kim, J. T., Lee, D. Y., Oh, T. S., & Lee, D. H. (2003). Characteristics of nitrile-butadiene rubber layered silicate nanocomposites with silane coupling agent. *Journal of Applied Polymer Science, 89*(10), 2633–2640.
Kittur, F. S., Haris, K. V., Udaya, K., & Tharanathan, R. N. (2002). Characterization of chitin, chitosan and their carboxymethyl derivatives by differential scanning calorimetry. *Carbohydrate Polymers, 49*, 185–193.
Lim, L. Y., & Wan, S. C. (1995). Heat treatment of chitosan films. *Drug Development and Industrial Pharmacy, 21*, 839–846.
Martínez-Romero, D., Alburquerque, N., Valverde, J. M., Guillén, F., Castillo, S., Valero, D., et al. (2006). Postharvest sweet cherry quality and safety maintenance by *Aloe vera* treatment: a new edible coating. *Postharvest Biology and Technology, 39*, 93–100.
McHugh, T. H., Avena-Bustillos, R. J., & Krochta, J. M. (1993). Hydrophilic edible film: Modified procedure for water vapor permeability and explanation of thickness effects. *Journal Food Science, 58*, 899–903.
Miranda, P. S., Garnica, O., Lara, V., & Cárdenas, G. (2004). Water vapor permeability and mechanical properties of chitosan composite films. *Journal of the Chilean Chemical Society, 49*(2), 173–178.
Muzzarelli, R. A. A., Isolati, A., & Ferrero, A. (1974). *Chitosan membranes: Ion exchange and membranes (p.193), Vol. 1.* London: Gordon and Breach Science Publishers.
Nunthanid, J., Puttipipatkhachorn, S., Yamamoto, K., & Peck, G. E. (2001). Physical properties and molecular behavior of chitosan films. *Drug Development and Industrial Pharmacy, 27*(2), 143–157.
Park, S. Y., Marsh, K. S., & Rhim, J. W. (2002). Characteristics of different molecular weight chitosan films affected by the type of organic solvents. *Journal of Food Science, 67*(1), 194–197.
Rhim, J., Hong, S., Park, H., & Perry, K. W. (2006). Preparation and characterization of chitosan-based nanocomposite films with antimicrobial activity. *Journal of Agricultural and Food Chemistry, 54*, 5814–5822.
Ribeiro, C., Vicente, A., Teixeira, J. A., & Miranda, C. (2007). Optimization of edible coating composition to retard strawberry fruit senescence. *Postharvest Biology and Technology, 44*, 63–70.
Sinha, S., & Okamoto, M. (2003). Polymer/layered silicate nanocomposites: a review from preparation to processing. *Progress in Polymer Science, 28*, 1539–1641.
Xu, Y., Ren, X., & Milford, A. (2006). Chitosan/clay nanocomposite film preparation and characterization. *Journal of Applied Polymer Science, 99*, 1684–1691.
Yano, K., Usuki, A., & Okad, A. (1997). Synthesis and properties of polyimide-clay hybrid films. *Journal of Polymer Science, Part A: Polymer Chemistry, 35*, 2289–2294.

Nomenclature

WVP: water vapor permeability
WS: water solubility
MC: moisture content
O_2P: oxygen permeability
CO_2P: carbon dioxide permeability
TS: tensile strength
E: elongation-at-break
q: chitosan concentration (% w/v)
c: clay concentration (% w/w chitosan)